Viscoelastic properties of a liquid-crystalline monomer and its dimer

Gregory A. DiLisi and Charles Rosenblatt*
Department of Physics, Case Western Reserve University, Cleveland, Ohio 44106-7079

Anselm C. Griffin
Melville Laboratory for Polymer Synthesis, University of Cambridge, Cambridge CB2 3RA, England

Uma Hari
Department of Chemistry, University of Southern Mississippi, Hattiesburg, Mississippi 39401
(Received 11 February 1991; revised manuscript received 15 October 1991)

Quasielastic-light-scattering measurements are reported for a dialkoxyphenylbenzoate monomer and its dimer in their respective nematic phases. The splay and twist elastic moduli of the dimer are found to be nearly independent of molecular length. The dimer's bend modulus, however, shows an anomalous increase with decreasing temperature well below the nematic-isotropic phase transition. Monomer viscosities are consistent with typical literature values, although $\gamma_1/\eta_{\text{splay}}$ and η_{bend} seem to be larger than expected for the dimer, where γ_1 is the twist viscosity. The results are discussed in terms of viscoelastic properties of semiflexible rods. The elastic properties in particular are in good agreement with a recent model by Terentjev and Petschek (unpublished).

PACS number(s): 61.30.Eb

Over the past 20 years, slow but steady progress has been made in the development of a comprehensive molecular understanding of liquid-crystalline viscous and elastic properties. The earliest models were based on either dispersive forces [1] or hard-core repulsions [2,3]; these models, moreover, were valid exclusively for rigid rods. The consequences of such limitations were demonstrated by de Jeu and Claassen [4], who showed that an increase in the length of the flexible terminal alkyl chains can lead to a decrease in the ratio of K_{33}/K_{11}, where K_{33} is the bend and K_{11} the splay elastic constant. More recent models [5,6] involving mixed attractive and repulsive interactions have generally met with more success, although these tend to involve a large number of parameters, making simple comparisons with experiment quite difficult.

During this period attention has also focused on elastic constants of oligomers and polymers. Terentjev and Petschek, for example, have developed a model [7] specifically for monomers and dimers that accounts for both attractive and repulsive interactions, as well as spacer flexibility. Using physically reasonable fitting parameters, predictions of their model are in good agreement with the experimental results reported herein. Others have considered [8,9] the elasticity of semiflexible main chain *polymers* in terms of entropic effects. For rigid rods, Lee and Meyer [10] have used a modified Onsager approach [11] to calculate both elastic constants and viscosities of aqueous solutions of rigid rods. Experimental results on tobacco mosaic virus (TMV) and polybenzyl glutamate (PBG) particles were remarkably successful [12–16], even demonstrating the crossover behavior of the bend elastic constant as the molecular length exceeds its persistence length, which characterizes the rigidity. Recently attempts have been made to model this crossover behavior from rigid to flexible molecules in terms of excluded-volume interactions [17]; experimental verification awaits.

In terms of rheological properties, fewer results have appeared on both the experimental and theoretical fronts. Several microscopic models were introduced during the past ten years [18,19], although their approximations tend to result in contributions to some of the Leslie coefficients which are not expressible in terms of microscopic parameters. Attempting to address this issue, Osipov and Terentjev developed a theory [20] that describes the microscopic stress tensor in terms of moments of inertia and intermolecular interaction potentials. Experimentally, the Osipov-Terentjev theory was examined by Wu and Wu [21], who fitted their measured twist viscosities γ_1 so as to extract, among other things, the activation energy and the mean-field interaction parameter.

In light of this extensive interest in the molecular origins of viscoelastic properties, we have performed a series of quasielastic light-scattering measurements on a particularly interesting system so as to investigate these properties as a function of molecular dimensions in the short-chain limit. We have chosen two molecules: the nearly symmetric monomer 4,4'-dipentyloxyphenly benzoate, called 5OO5, ($C_5H_{11}OC_6H_4COOC_6H_4OC_5H_{11}$) and its associated dimer, which consists of two monomers (minus one hydrogen each) attached end to end. In previous studies of this pair we have explored the spacer confirmation of the dimer in the isotropic phase near the nematic transition [22] and, by means of the Fréedericksz technique, measured the splay elastic constant as a function of temperature [23]. Since both x-ray and NMR measurements indicate that the spacer group in a very

large fraction of the dimers is fully extended in the nematic phase [24–26], the aspect ratio L/d of the dimer can be considered to be twice that of the monomer. Here L is the length and d the diameter of the molecule. In this light such a system *might* represent a convenient test of those theories in which the aspect ratio plays an important role. (One must nevertheless take care to sort out spurious effects involving both flexibility and temperature variations in the nematic order parameter S, which are not accounted for in many of the models.) Along these lines rather elegant experiments have been carried out by Meyer and co-workers [12–16] on aqueous suspensions of elongated polyelectrolytes. Our system, however, differs in two important respects. First, 5OO5 and its dimer are dense liquids, unlike the far more dilute polyelectrolytes. In addition, owing to the small molecular size and higher density, long-range attractive interactions may be important, rendering the monomer and dimer systems thermal; the order parameter therefore becomes a function of temperature. Finally, one important caveat remains: based upon the results of Ref. [4], molecules containing alkyl chains are likely to be less than completely rigid, a conclusion that superficially appears to be inconsistent with the NMR and x-ray results on this particular system. We shall nevertheless see that even weak flexibility plays a major role in the viscoelastic properties of these materials, and cannot be ignored. Given these difficulties, then, it is clear that direct comparison of our results with many of the theoretical models is inappropriate. Therefore, we shall ultimately concentrate our discussion on the model of Terentjev and Petschek [7], which applies specifically to our system.

The basis for determining both the viscous and elastic properties of nematics liquid crystals is well established [27–29]. Light scattered by angular fluctuations of the director $\mathbf{n}$ is composed of two modes corresponding to bend-splay (mode-1) and bend-twist (mode-2) deformations. For the undistorted director $\mathbf{n}_0$ parallel to the z axis, the differential scattering cross section per unit volume is given by

$$\frac{d\sigma}{d\Omega}=\frac{\pi\Delta\epsilon^2}{\lambda^2}k_BT\sum_{\nu=1,2}\frac{(i_\nu f_\parallel+i_\parallel f_\nu)^2}{K_{33}q_\parallel^2+K_{\nu\nu}q_\perp^2}\ , \tag{1}$$

where k_B is Boltzmann's constant, T is temperature, λ is the wavelength of light, $\Delta\epsilon$ the anisotropy in the optical dielectric tensor, and K_{11}, K_{22}, and K_{33} are the splay, twist, and bend elastic constants, respectively. In addition, $\mathbf{q}$ corresponds to the difference between the incident and scattered wave vectors, and has components $q_\parallel$ parallel to $\mathbf{n}_0$ and $q_\perp$ in the plane perpendicular to $\mathbf{n}_0$. i_ν and f_ν are the components of the initial and final polarizations along the $\delta\mathbf{n}$ ($\equiv\mathbf{n}-\mathbf{n}_0$) directions for the two modes, formally defined as

$$i_\nu=\mathbf{e}_\nu\cdot i\ ,\quad f_\nu=\mathbf{e}_\nu\cdot\mathbf{f}\ ,$$

where

$$\mathbf{e}_2=\mathbf{n}_0\times\mathbf{q}/|\mathbf{n}_0\times\mathbf{q}|\ ,\quad \mathbf{e}_1=\mathbf{e}_2\times\mathbf{n}_0/|\mathbf{e}_2\times\mathbf{n}_0|\ .$$

By means of photon-correlation spectroscopy one can determine the relaxation frequencies Γ for the two director modes:

$$\Gamma_\nu(\mathbf{q})=\frac{(K_{33}q_\parallel^2+K_{\nu\nu}q_\perp^2)}{\eta_\nu(\mathbf{q})} \tag{2}$$

where the viscosities η_ν are given by

$$\eta_1(\mathbf{q})=\gamma_1-\frac{(q_\perp^2\alpha_3-q_\parallel^2\alpha_2)^2}{q_\perp^4\eta_b+q_\perp^2q_\parallel^2(\alpha_1+\alpha_3+\alpha_4+\alpha_5)+q_\parallel^4\eta_c} \tag{3}$$

and

$$\eta_2(\mathbf{q})=\gamma_1-\frac{\alpha_2^2q_\parallel^2}{q_\perp^2\eta_a+q_\parallel^2\eta_c}\ . \tag{4}$$

The quantities α_i refer to the five Leslie coefficients [30], γ_1 is the twist viscosity, and η_a, η_b, and η_c are the Miesowicz viscosities [31], which can be expressed in terms of the Leslie coefficients.

In our experiments we have utilized two configurations, which are described in detail elsewhere [32]. In the first configuration $q_\parallel=0$ and the scattering plane is perpendicular to $\mathbf{n}_0$ [Fig. 1(a)]. Thus, according to Eq. (1), the scattered light intensity I arises from the sum of two modes (splay and twist), the contribution of each determined by the scattering angle and optical polarization factors:

$$I\propto\frac{n_e^2\sin^2\phi}{K_{11}q_\perp^2}+\frac{(n_o-n_e\cos\phi)^2}{K_{22}q_\perp^2}\ , \tag{5}$$

where ϕ is the scattering angle *inside* the liquid crystal, and n_e and n_o are the extraordinary and ordinary refractive indices. In addition, the decay rates for the two

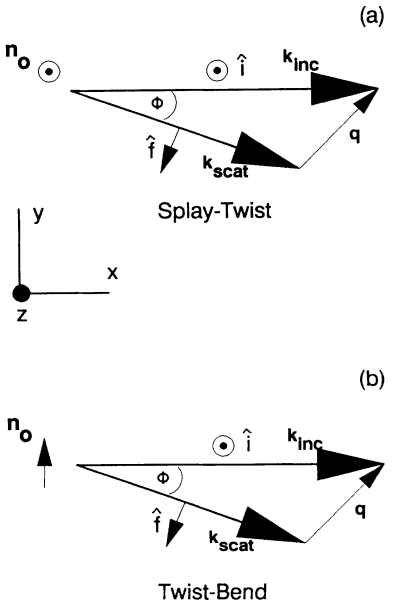

FIG. 1. Schematic representation of light-scattering geometry. Configuration (a) samples a combination of mode 1 and mode 2 with $q_\parallel=0$, corresponding to splay and twist. Configuration (b) samples mode 2 only, which corresponds to a mixture of twist and bend.

modes reduce to

$$\Gamma_1 = K_{11} q_\perp^2 / (\gamma_1 - \alpha_3^2/\eta_b) \equiv K_{11} q_\perp^2 / \eta_{\text{splay}} \quad (6)$$

and

$$\Gamma_2 = K_{22} q_\perp^2 / \gamma_1 \, . \quad (7)$$

In the second geometry $\mathbf{n}_0$ lies in the scattering plane [Fig. 1(b)]. Moreover, since $\delta\mathbf{n}$ for mode 1 also lies in the scattering plane, the polarization factor for a depolarized mode-1 experiment vanishes. Thus, the only contribution to Eq. 1 comes from mode 2 (bend-twist), such that $q_\parallel$ is associated with the bend component and $q_\perp$ with the twist component of the director distortion. The intensity is therefore given by

$$I \propto \frac{\cos^2\phi}{K_{33} q_\parallel^2 + K_{22} q_\perp^2} \, . \quad (8)$$

In addition, since only a single mode is sampled, only one decay rate $\Gamma_2(\mathbf{q})$ is present, and is given by Eq. (2) with $\nu = 2$.

The monomer and dimer were synthesized according to procedures described elsewhere [33–35]. Two pairs of glass microscope slides, cut to approximately 1×3 cm^2, were coated with nylon 6/6 and rubbed undirectionally. The slides were separated by Mylar spacers of nominal thickness 25 μm, and the filled sample cell was inserted in an insulated aluminum oven. The oven was temperature controlled to approximately 10 mK for the monomer and 25 mK for the dimer, using a proportional controller. The sample was illuminated with polarized light from a 1-W argon-ion laser operating at a wavelength of 5145 Å. Although the incident beam emerged from the oven through a glass window, the oven had a small ($\sim$3 mm diameter) movable hole through which the scattered light could emerge; in this way the scattered light was not susceptible to distortion, and the sample remained well insulated from air convection.

The scattering optics were based upon the model of Taratuta, Hurd, and Meyer [36]. The oven was placed on a microrotation stage having an angular resolution of approximately 5×10^{-5} rad. A Newport micro-optical rail, approximately 30 cm in length, was mounted radially on a separate concentric rotation stage having the same angular resolution, allowing for independent rotation of the sample and collection optics. Light emerging from the sample passed consecutively through an iris diaphragm, an analyzer, and a 2.5-cm focal length lens (L_1), all mounted in such a way as to allow for translation along three axes and rotation about two axes. The scattered light then entered a small aluminum box that housed a polished brass foil disk whose normal made a small angle ($\sim 15°$) with the incoming scattered light. The lens L_1 was positioned to create a variably sized real image of the sample volume on the brass disk, which could be viewed by an adjustable mirror-lens combination also housed in the aluminum box. Additionally, a 200-μm pinhole was bored through the center of the brass disk, which defined the actual sample volume probed by the detector. This arrangement allowed us to view the sample volume and, if dust or disclinations were present, allowed us to translate the sample (using a three-axis translator) so that scattered light from only a well-aligned portion of the sample would pass through the pinhole. This light then passed through a bellows into a second aluminum box of similar design and having a pinhole of approximately 350 μm. We were thus able to observe the scattered light and, in fact, adjust the position of the second box so that only one coherence area was sampled. The distance between pinholes was typically 15 cm. The scattered light then entered a single-mode optical fiber and emerged into a Thorn-EMI 9863B photomultiplier tube. After passing through a pulse amplifier-discriminator, the signal was input to a Brookhaven Instruments model BI-2030AT 136-channel digital autocorrelator for processing.

The advantages of this scattering arrangement, unfortunately, are somewhat offset by two drawbacks. First, since the image created by lens L_1 is inverted, the light entering the detector represents an additional spread in the scattered wave vector Δq over and above that which ordinarily would arise from the solid angle of the pinholes; for our apparatus this corresponds to $\pm\frac{1}{4}°$. Owing to the smallness and symmetry of Δq, and in light of the single exponential behavior of the time autocorrelation function from monodisperse latex particles in earlier tests, this was not deemed a problem. Second, although each point at the sample maps to a point at the first pinhole, the lens does not reconstruct an exact *three-dimensional* image. Thus, not only does the effective scattering volume become an extremely complex function of scattering angle, pinhole size, and focal length of L_1, but so also does the effective solid angle of the detector [cf. Eq. (1)]. In consequence it is necessary to calibrate the measured intensity as a function of scattering angle against a standard. This will be discussed below.

In order to experimentally establish $\mathbf{q}$, it was necessary to know the refractive indices of the materials. To that end we measured both the average index n_{iso} in the isotropic phase and the birefringence Δn as a function of temperature in the nematic phase. It is easy to show that the extraordinary index n_e is

$$n_e = \tfrac{2}{3}\Delta n + (n_{\text{iso}}^2 - 2\Delta n^2/9)^{1/2} \, ,$$

and the ordinary index $n_o = n_e - \Delta n$. To determine n_{iso} a 1-cm path-length cuvette was placed on a precision rotation stage and filled with either monomer or dimer. Light at wavelength $\lambda = 5145$ Å passed through the cuvette and was displaced as the sample was rotated. By measuring the displacement distance (using a micrometer mounted pinhole) and using Snell's Law corrected for the windows of the cuvette, n_{iso} was determined for the monomer ($n_{\text{iso}} = 1.539 \pm 0.005$) and the dimer ($n_{\text{iso}} = 1.534 \pm 0.01$). So as to determine the birefringences in the nematic phase as a function of temperature, thin cells (typically about 10 μm) were made and the thicknesses determined to 0.01 μm using an interferometric technique [37]. Δn vs $T - T_{N-I}$ was then measured using a calibrated Pockels cell, and the results are shown in Fig. 2. (T_{N-I}, the first-order nematic-isotropic phase-transition temperature, is 79.6 °C for the monomer and 149.0 °C for the dimer.) The ordinary and

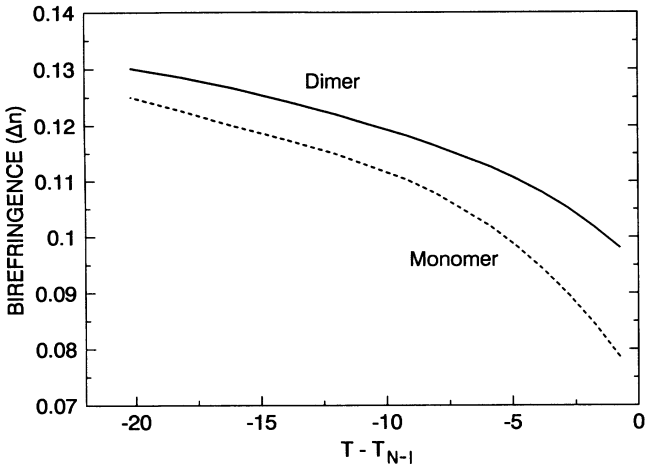

FIG. 2. Birefringence of the monomer (dashed line) and dimer (solid line) vs reduced temperature at wavelength $\lambda = 5145$ Å.

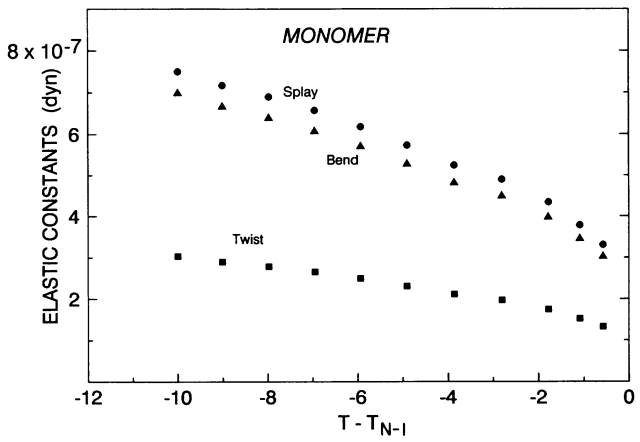

FIG. 3. Elastic constants vs reduced temperature for the monomer. ● corresponds to K_{11} (splay), ■ to K_{22} (twist), and ▲ to K_{33} (bend). Error bars are discussed in detail in the text.

extraordinary refractive indices were extracted accordingly.

Armed with n_e and n_o, we first performed measurements in the splay-twist geometry with $\mathbf{n}_0$ perpendicular to the scattering plane [Fig. 1(a)]. The incident polarization was extraordinary (along the z axis), and the scattered polarization was in the xy plane, corresponding to the VH depolarized geometry. Measurements were made at two scattering angles θ (defined in the laboratory frame) for each material at each temperature: $\theta = 10°$ and $\theta = \theta_{\text{splay}}$. Note that θ was determined from the internal scattering angle ϕ by means of Snell's law. At 10° the polarization factors in Eq. (1) for both splay and twist modes are of comparable magnitude; at the special angle θ_{splay}, typically 30°–35°, the polarization factor vanishes for the twist mode, and only splay is sampled. θ_{splay} is, of course, a function of the refractive indices and thus temperature, and is determined by the condition that $\mathbf{q}(=q_\perp)$ be perpendicular to f_2 [cf. Eq. (1)]. At each of the two scattering angles the correlator gathered data for several minutes in order to build up a smooth correlation function. The intensities $I(\theta)$ were taken as the total number of counts divided by the corresponding collection times, multiplied by an angular dependent scaling factor, to be described in the next paragraph. Since $I(\theta = 10°)$ involves both splay and twist and $I(\theta_{\text{splay}})$ involves splay exclusively, the ratio K_{22}/K_{11} could be extracted from the ratio of the two intensities [cf. Eq. (5)]. Moreover, using the Fréedericksz technique, we had previously obtained absolute values for K_{11} versus temperature for the two species [9], and thus were now able to extract the absolute twist elastic constant as well. The twist and splay elastic constants (as well as K_{33}, to be described below) versus reduced temperature are shown in Fig. 3 for the monomer and Fig. 4 for the dimer.

As discussed above, owing to the change in the image caused by lens L_1, the measured intensities must first be scaled by a complicated geometric factor before their ratios are taken at the two different angles θ and θ_{splay}. To establish this angular dependent factor, we first performed the experiment on pentylcyanobiphenyl (5CB), obtained from BDH Ltd. and used without further purification. Eight intensity measurements were made at angles between 10° and 40°, as well as at the appropriate angle θ_{splay} for 5CB. For each angle the measured intensity was scaled by a suitable factor so that the elastic constant ratio K_{22}/K_{11} resulting from the intensity ratio $I(\theta)/I(\theta_{\text{splay}})$ corresponded to that obtained in Ref. [32]. As expected, the intensity scaling factor at each angle was found to be independent of temperature. As an additional check, we also studied octylcyanobiphenyl (8CB), again obtained from BDH Ltd. Using the intensity scaling factors obtained above, we were able to reproduce the elastic constant ratios found by Madhusudana and Pratibha [38] extremely accurately. Moreover, using the Fréedericksz technique, we had previously obtained absolute values for K_{11} for the monomer [23]. In addition, we are able to extract K_{33} for the monomer from our previously published Fréedericksz data [39]. Again we find good agreement for K_{11}/K_{33} between our light-scattering measurements based upon the *scaled* intensities and these Fréedericksz results. In light of all this evidence, we are convinced of the efficacy of our scaling procedure.

In order to obtain viscosity information, we note that at θ_{splay} only a single mode is present, and therefore only one exponential decay exists in the correlation function. For a homodyning experiment we then fit a single decay time $\tau_1 = 1/2\Gamma_1$ to the data, allowing us to extract η_{splay} from Eq. (6). Based upon the smallness of the second and higher coefficients in a followup cumulant fit, the single decay was deemed appropriate at θ_{splay}. It was more difficult to extract γ_1. At $\theta = 10°$ the intensity-intensity autocorrelation function is the square of the sum of two exponentials involving four parameters: two decay times and two coefficients, where the base line was obtained from the correlator's six delay channels. In order to reduce the number of fitting parameters we note that, since the two elastic constants K_{11} and K_{22} have already been obtained above, the *ratio* of the coefficients of the two exponentials is also known [from Eq. (5)]. In addition, since η_{splay} has been obtained, τ_1 can be obtained at $\theta = 10°$ by scaling Eq. (6) to the appropriate value of $q_\perp$.

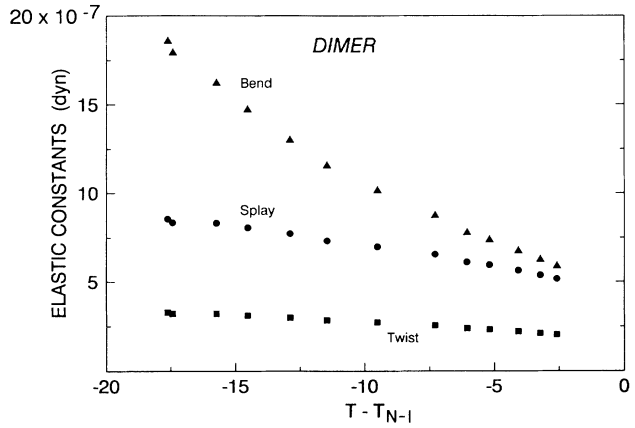

FIG. 4. Same as Fig. 2, except for the dimer.

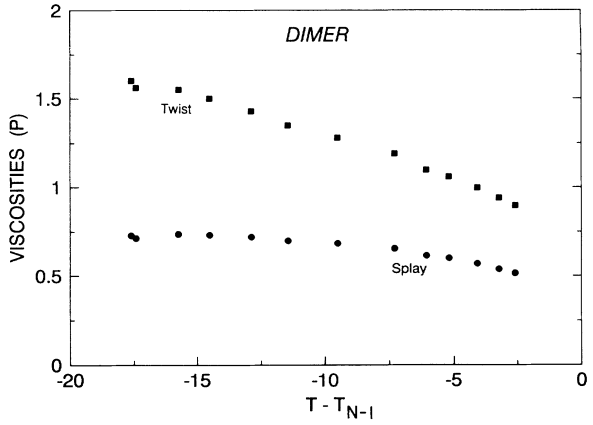

FIG. 6. Same as Fig. 4, except for the dimer.

Thus, a two-parameter fit was performed to the correlation function at 10°, allowing us to extract τ_2. Finally, taking $\Gamma_2=1/2\tau_2$, γ_1 was extracted from Eq. (7). Results for η_{splay} and γ_1 are shown in Figs. 5 and 6 for the monomer and dimer, respectively.

We now turn to the second geometry in which $\mathbf{n}_0$ lies in the scattering plane [Fig. 1(b)]; this geometry measures a pure mode (mode 2) corresponding to a mixture of bend and twist. Physically the sample was rotated by 90° about the x axis, such that the incident polarization was perpendicular to $\mathbf{n}_0$. This is again a VH experiment, although the depolarized scattering is now ordinary to extraordinary.

Measurements were made in the bend-twist geometry at $\theta=10°$ in the laboratory frame and also at the temperature-dependent special angle $\theta=\theta_{\text{bend}}$. Since this geometry involves only one mode (mode 2), the polarization factor in Eq. (1) does not distinguish twist from bend; rather, the wave vector $\mathbf{q}$ associated with scattering at 10° decomposes into $q_\parallel$ associated with bend and $q_\perp$ associated with twist [cf. Eq. (8)]. In addition, there exists a scattering angle θ_{bend} such that $q_\perp=0$, and the scattered light involves only bend distortions. As was the case with splay-twist, intensity-intensity autocorrelation functions were made for the monomer and dimer at both angles as a function of temperature. At a given temperature for a given species the ratio K_{33}/K_{22} was extracted from the ratio $I(\theta=10°)/I(\theta_{\text{bend}})$ using Eq. (8). Since the twist elastic constant was determined above, we were able to extract absolute values of K_{33} versus temperature; results are given in Figs. 3 and 4. Additionally, the correlation functions taken at θ_{bend} were fitted to a single exponential decay, from which Γ_2 was extracted. From Eqs. (2) and (4) we find

$$\Gamma_2(q_\perp=0)=K_{33}q_\parallel^2/(\gamma_1-\alpha_2^2/\eta_c)$$
$$=K_{33}q_\parallel^2/\eta_{\text{bend}}\ . \tag{9}$$

Thus, analogous to η_{splay}, an effective $q_\parallel$-independent bend viscosity was extracted for both monomer and dimer, and is shown in Figs. 7 and 8.

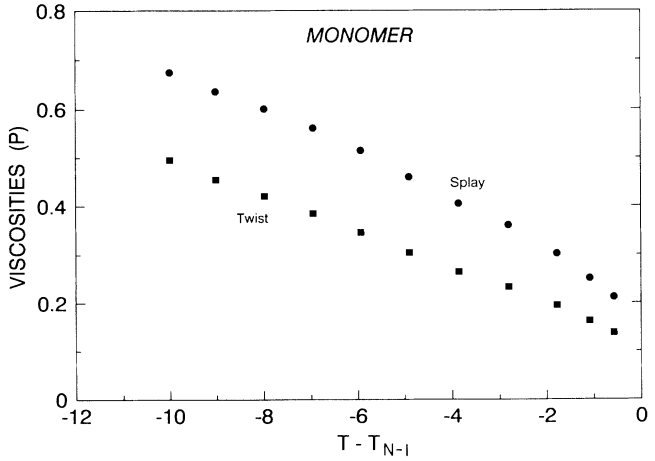

FIG. 5. Splay viscosity η_{splay} (●) and twist viscosity γ_1 (■) vs temperature for the monomer. Error bars are discussed in the text. Note that the negative curvature is an artifact of the data smoothing procedure; a positive curvature is within the error bars. See text.

Before discussing the results, we first discuss our data analysis and resulting error bars. K_{11} was obtained previously from Fréedericksz measurements [23], with overall error bars of about 10%. Approximately 3% of that error corresponds to scatter, and the remainder arises from uncertainties in such quantities as the magnetic susceptibility anisotropy $\Delta\chi$, which was taken from the literature [25]. A few points need to be mentioned. Recently we discovered a small error in the thickness of our dimer cell used in Ref. [23], resulting in a systematic error in K_{11} for the dimer; instead of 62 ± 1 μm, the thickness was actually 57 ± 1 μm. Values of K_{11} reported herein reflect the correct sample thickness. In addition, we have recently investigated the anchoring strength of both monomer and dimer in the homogeneous geometry at a buffed polyimide-coated substrate. The results, which are reported elsewhere [40], indicate that although the dimer anchoring is quite strong, the weaker anchoring associated with the monomer may have resulted in a small but measurable decrease in the Fréedericksz threshold fields [41] reported in Ref. [23]. If the anchoring characteristics at a nylon surface are similar, the values of K_{11} for the monomer reported in Ref. [23] and used in this work

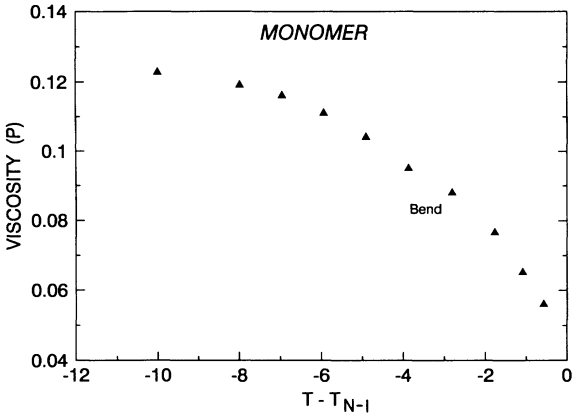

FIG. 7. Bend viscosity η_{bend} vs temperature for the monomer. Error bars are discussed in the text.

may be low by as much as 15%. This relative error would ultimately propagate to all the elastic moduli and viscosities, although the general and specific conclusions drawn in this work would not be affected by such a small error.

In the splay-twist geometry the intensity ratios $I(\theta=10°)/I(\theta_{\text{splay}})$ as a function of temperature were determined to within a few percent, which corresponds to an error of less than 10% for ratios of K_{22}/K_{11}. These ratios (for the monomer and dimer) were fitted versus temperature to a straight line. The previously obtained values of K_{11} [23] were then multiplied by the *fitted* ratios K_{22}/K_{11} at those temperatures to obtain K_{22}. Thus the overall error associated with K_{22} in Figs. 3 and 4 is somewhat less than 20%. It is important to bear in mind that most of the experimental scatter does *not* appear in the actual figures. This is because we have linearly fitted (and thereby smoothed) the measured values of K_{22}/K_{11}, which *do* contain substantial scatter, in order to obtain K_{22} absolutely. Nevertheless, when interpreting the elastic and viscosity figures, one must be aware that not insignificant error bars exist.

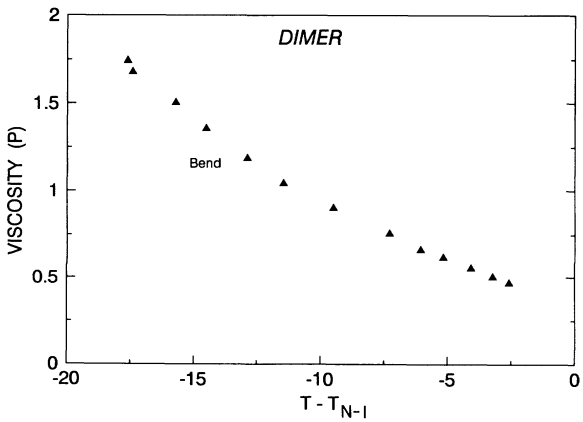

FIG. 8. Same as Fig. 6, except for the dimer.

In the bend-twist geometry the intensity errors were comparable to those of K_{22}/K_{11}, again leading to an error somewhat smaller than 10% in the ratio K_{33}/K_{22}. Again this ratio was fitted to a straight line for both monomer and dimer, and the fitted values were multiplied by the values of K_{22} versus temperature obtained above; the overall error associated with K_{33} was in the neighborhood of 25%. It must be emphasized, however, that approximately 7% of the error associated with each of the elastic constants is *not* due to scatter, but rather is systematic and arises from the literature values of the magnetic susceptibility and uncertainty in the sample thicknesses used in the earlier Fréedericksz measurements.

Interpolation for the viscosities was done similarly. The primary source of error for the viscosities was uncertainty in the elastic constants [see Eqs. (6), (7), and (9), and the preceeding two paragraphs], since the decay-time components at both θ_{splay} and θ_{bend} were easily reproducible to within 1% or 2%. γ_1, however, involves a double exponential fit in which the ratio K_{22}/K_{11} is needed for one of the relaxation coefficients. Thus the uncertainty in this ratio appears twice in obtaining γ_1: once through the elastic constant K_{22} [cf. Eq. (7)] and once through the double exponential fit. As a result, γ_1 can be expected to have a large uncertainty. Again, as with the case of the elastic constants, it is necessary to keep in mind that the figures as drawn do not reflect the actual scatter, and that a part of the absolute error arises from systematic error in $\Delta\chi$.

Given the caveats outlined above, we now discuss our results. Several features are immediately obvious in Figs. 3 and 4. First, the splay elastic constants for monomer and dimer are similar for corresponding reduced temperatures. These results, of course, are taken from previous Fréedericksz measurements [23]. In that paper, moreover, we found that the ratios K_{11}/S^2 are nearly identical for both species and exhibit only a very weak dependence on temperature. As is the case with K_{11}, the twist elastic constants versus reduced temperature for monomer and dimer are also quite similar, again being nearly equal when scaled by the nematic order parameter [26]. Only the bend elastic constants show marked differences, increasing significantly (relative to K_{11}) for the dimer, especially at lower temperatures. In fact, not only does K_{33} cross over from being smaller than K_{11} in the monomer to being larger than K_{11} in the dimer, but $|d(K_{33})/dT|$ for the dimer also seems to increase with reduced temperature well into the nematic phase. Such behavior is often associated with a nearby smectic-A phase, although corresponding behavior was not observed for the twist elastic constant. Moreover, a nematic to crystalline transition occurs at approximately $T_{N-I}-25\,°\text{C}$, well below the region shown in Fig. 4. Although one cannot discount the possibility that this behavior is an artifact arising from the relatively large uncertainty in determining K_{33}, we do not feel that this is likely, given that the uncertainty in K_{33} tends to represent point-by-point scatter rather than systematic error. We therefore

suspect that this effect is real.

Monomers and semiflexible dimers and tetramers have been treated theoretically by Terentjev and Petschek [7]. (Since approximations such as nonflexibility, which are associated with some of the other models, tend to be physically unrepresentative of our system, those models will not be considered here. Rather, we will concentrate on the model of Ref. [7].) Terentjev and Petschek considered anisotropic mesogens that interact via both an attractive part of the potential (including isotropic and anisotropic contributions) and a hard-core repulsive part. This repulsive part contributes to both the attraction cutoff on the molecule surface and to the packing (translational) entropy of the system. In addition, they included both a stiffness parameter Ω for the spacer (which is determined by its effective bending energy, $\Omega \sim E_B / k_B T$) and a "bare" angle θ_0 between the mesogens which, for our dimer, is approximately equal to zero. (The case $\theta_0 \neq 0$ corresponds to a kinked dimer—for example, a dimer that contains an odd number of methylene units in the spacer. The model predicts very different results for such a molecule, which are consistent with our recent experimental results for a dimer with nine methylene units in the spacer. This work is planned to be published elsewhere [42].) Thus, with the inclusion of flexibility, the dimer in a sense consists of two mesogens separated by a semiflexible string.

For both the monomer and the rigid dimer (in the limit $\Omega \rightarrow \infty$), Terentjev and Petschek obtained elastic moduli with the correct magnitudes. Moreover, they found that the splay and twist elastic constants remain almost unchanged with molecular length; this surprising result turns out to be completely consistent with our data. Also consistent with our results and, in fact, with the results of most rigid rod models as well, they found $K_{22}/K_{11} \sim \frac{1}{3}$ for both the monomer and dimer. In addition, they found that K_{33}/K_{11} exhibits a temperature dependence similar to that observed experimentally, and shown in Fig. 4. This behavior, which becomes more pronounced with an increasing number of mesogens in the molecule, arises from the order-parameter dependence of K_{33}, such that K_{33} diverges as $(1-S)^{-1}$. Not limiting themselves to rigid spacers, Terentjev and Petschek also numerically examined finite values of Ω, which would correspond to some degree of spacer flexibility. For physically reasonable values of Ω, i.e., $1 < \Omega < 25$, they found results qualitatively similar to those of the rigid dimer. (Note that $\Omega \sim 6$ corresponds approximately to the $[CH_2]_{10}$ spacer [43].) More specifically, they found that the temperature dependence of K_{33}/K_{11} remains, although the divergence at lower temperatures tends to be weaker. This result is in good quantitative agreement with our data.

The picture that emerges has a number of discernable features. First, the dimer cannot be considered rigid, and is too short to be analyzed in terms of semiflexible polymer models. As the orientational order increases deep into the nematic phase, the bend elasticity tends to grow rapidly as the order parameter approaches unity. Finally, we have an interesting dichotomy: from the standpoint of spacer-conformation populations and such quantities as the latent heat near the nematic-isotropic phase transition [26], the dimer is, for all intents and purposes, rigid. On the other hand, in terms of elastic moduli, the dimer *must* be considered partially flexible. [We note as an aside that the idea of a highly ordered yet partially flexible spacer is reinforced by the observation that dimers having shorter spacers (two methylene units) exhibit a smectic-A phase as well as a nematic phase [44]. For longer spacer dimers the small degree of flexibility is likely responsible for eliminating the smectic-A phase.]

The viscosity data (cf. Figs. 5–8) are even more difficult to interpret. For the monomer, both η_{splay} and γ_1 are comparable to each other, and over the entire temperature range are approximately four to six times η_{bend}. These results are completely consistent with those for other low-molecular-weight materials [28,45], both in relative terms (e.g., $\gamma_1/\eta_{\text{bend}}$) as well as absolute values. The only troubling issue is that γ_1 appears to be smaller than η_{splay}. The difference is likely an artifact of the multiexponential fit, and is characteristic of the sort of error bars expected. On the other hand, for the dimer the results are considerably different. First, the magnitude of the splay viscosity is comparable to its monomer counterpart, and that of the twist viscosity is up to twice that of the monomer at comparable reduced temperatures. Clearly the tendency of the dimer to be more viscous than the monomer is largely offset by the higher dimer transition temperature and noncommitant Arrhenius behavior of the viscosites. Second, we find that $\gamma_1 > \eta_{\text{splay}}$ by a more substantial amount than one ordinarily finds in shorter mesogens. Finally, η_{bend} for the dimer is much larger than for the monomer, and is of the same order as, and even larger than, η_{splay}. (η_{bend} also appears to be larger than γ_1 well below T_{N-I}, although we feel that this is an artifact of the fitting.)

Meyer and co-workers have extensively studied the issue of viscosities in elongated polyelectrolytes [11–16]. Our system differs from theirs in several important respects, however: the aspect ratios of our monomer and dimer are relatively small, our molecules are thermal, and they tend to be far more flexible than the polyelectrolytes. These differences give rise to very different sorts of viscous behavior for our materials. For example, the ratio $\gamma_1/\eta_{\text{bend}}$ for the dimer is not only much smaller than that of PBG, but also tends toward the opposite direction as a function of L/d. It is clear, then, that our system is considerably more complex than the lyotropic nematics liquid crystals, and cannot adequately be described by viscous theories of long rigid, or even long semiflexible, molecules. Thus, despite the fact that one can stretch the limits of applicability of models such as those of Osipov and Terentjev [20] to achieve results qualitatively consistent with experiment, utilization of such models is inappropriate, owing to, among other things, the dimer's inherent flexibility. It is nevertheless hoped that our experimental results will encourage theoretical work on the visocus properties of such molecules.

Throughout our discussion we have attempted to interpret our results in terms of appropriate models for rigid

or semiflexible molecules. None of these models, however, properly accounts for effects such as permanent dipolar interactions, packing, and short-range order, which are important to dense systems of small molecules such as ours. In this light our interpretations must contain a caveat: the disagreement of our results with theory may be due to the inherent incompleteness of any theoretical model. By choosing this relatively simple monomer-dimer system we have attempted to minimize these ancillary effects; nevertheless, it is unlikely that we have entirely eliminated them.

The authors wish to thank Dr. Eugene Terentjev, Dr. Rolfe Petschek, Dr. Philip Taylor, Dr. Sin-Doo Lee, Dr. Alexander Jamieson, and Dr. Kenneth Singer for useful discussions. We also wish to thank Shih Song Cheng for purification of the monomer. This work was supported by the National Science Foundation Division of Materials Research, under Grants No. DMR-8901854 (C.R.) and No. DMR-8417834 (A.C.G.)

---

*Also at Department of Macromolecular Science, Case Western Reserve University.

[1] J. Nehring and A. Saupe, J. Chem. Phys. **56**, 5527 (1972).
[2] J. P. Straley, Phys. Rev. A **8**, 2181 (1973).
[3] R. G. Priest, Phys. Rev. A **7**, 720 (1973).
[4] W. H. de Jeu and W. A. P. Claassen, J. Chem. Phys. **67**, 3705 (1977).
[5] W. M. Gelbart and A. Ben-Shaul, J. Chem. Phys. **77**, 916 (1982).
[6] E. Govers and G. Vertogen, Liq. Cryst. **2**, 31 (1987).
[7] E. M. Terentjev and R. G. Petschek (unpublished).
[8] P. G. de Gennes, in *Polymer Liquid Crystals*, edited by A. Ciferri, W. R. Krigbaum, and R. B. Meyer (Academic, New York, 1982).
[9] R. B. Meyer, in *Polymer Liquid Crystals* (Ref. [8]).
[10] S.-D. Lee and R.B. Meyer, J. Chem. Phys. **84**, 3443 (1986).
[11] L. Onsager, Ann. N.Y. Acad. Sci. **51**, 627 (1949).
[12] S.-D. Lee and R. B. Meyer, Phys. Rev. Lett. **61**, 2217 (1988).
[13] S.-D. Lee and R. B. Meyer, Liq. Cryst. **7**, 15 (1990).
[14] V. G. Taratuta, A. J. Hurd, and R. B. Meyer, Phys. Rev. Lett. **55**, 246 (1985).
[15] R. B. Meyer, F. Lonberg, V. Taratuta, S. Fraden, S.-D. Lee, and A. J. Hurd, Faraday Disc. Chem. Soc. **79**, 125 (1985).
[16] V. G. Taratuta, F. Lonberg, and R. B. Meyer, Phys. Rev. A **37**, 1831 (1988).
[17] T. Odijk, Liq. Cryst. **1**, 553 (1986).
[18] A. C. Diogo and A. F. Martins, Mol. Cryst. Liq. Cryst. **66**, 133 (1981).
[19] N. Kuzuu and M. Doi, J. Phys. Soc. Jpn. **52**, 3486 (1983).
[20] M. A. Osipov and E. M. Terentjev, Z. Naturforsch. **44**, 785 (1989).
[21] S.-T. Wu and C.-S. Wu, Phys. Rev. A **42**, 2219 (1990).
[22] C. Rosenblatt and A. C. Griffin, Macromolecules **22**, 4102 (1989).
[23] G. A. DiLisi, C. Rosenblatt, A. C. Griffin, and U. Hari, Liq. Cryst. **8**, 437 (1990).
[24] H. H. Chin, L. V. Azaroff, and A. C. Griffin, Mol. Cryst. Liq. Cryst. **157**, 443 (1988).
[25] D. Y. Yoon, S. Bruckner, W. Volksen, J. C. Scott, and A. C. Griffin, Faraday Disc. Chem. Soc. **79**, 41 (1985).
[26] G. Sigaud, D. Y. Yoon, and A. C. Griffin, Macromolecules **16**, 875 (1983).
[27] Orsay Liquid Crystal Group, J. Chem. Phys. **51**, 816 (1969).
[28] Orsay Liquid Crystal Group, Phys. Rev. Lett. **22**, 1361 (1969).
[29] P. G. de Gennes, *The Physics of Liquid Crystals* (Clarendon, Oxford, England, 1975).
[30] F. M. Leslie, Q. J. Appl. Math **19**, 357 (1966).
[31] M. Miesowicz, Bull. Int. Akad. Polon. Sci. Lett. Ser. A **28**, 225 (1936).
[32] D. Gu, A. M. Jamieson, C. Rosenblatt, D. Tomazos, M. Lee, and V. Percec, Macromolecules **24**, 2385 (1991).
[33] A. C. Griffin and E. T. Samulski, J. Am. Chem. Soc. **107**, 2975 (1985).
[34] A. C. Griffin, S. L. Sullivan, and W. E. Hughes, Liq. Cryst. **4**, 667 (1989).
[35] A. C. Griffin and S. J. Havens, J. Polym. Sci. Polym. Phys. Ed. **19**, 969 (1981).
[36] V. G. Taratuta, A. J. Hurd, and R. B. Meyer, Rev. Sci. Instrum. **55**, 751 (1984).
[37] C. Rosenblatt, J. Phys. (Paris) **45**, 1087 (1984).
[38] N. V. Madhusudana and R. Pratibha, Mol. Cryst. Liq. Cryst. **89**, 249 (1982).
[39] G. A. DiLisi, C. Rosenblatt, A. C. Griffin, and U. Hari, Liq. Cryst. **7**, 353 (1990).
[40] G. A. DiLisi, C. Rosenblatt, R. B. Akins, A. C. Griffin, and U. Hari, Liq. Cryst. **11**, 63 (1992).
[41] A. Rapini and M. Papoular, J. Phys. (Paris) Colloq. **30**, C4-54 (1969).
[42] G. A. DiLisi, C. Rosenblatt, and A. C. Griffin, J. Phys. (Paris) (to be published).
[43] E. M. Terentjev, R. G. Petschek, and C. Rosenblatt (unpublished).
[44] A. C. Griffin (unpublished).
[45] H. Kneppe, F. Schneider, and N. K. Sharma, J. Chem. Phys. **77**, 3203 (1982).